

Photochemical & Photobiological Sciences

Accepted Manuscript



This is an *Accepted Manuscript*, which has been through the Royal Society of Chemistry peer review process and has been accepted for publication.

Accepted Manuscripts are published online shortly after acceptance, before technical editing, formatting and proof reading. Using this free service, authors can make their results available to the community, in citable form, before we publish the edited article. We will replace this *Accepted Manuscript* with the edited and formatted *Advance Article* as soon as it is available.

You can find more information about *Accepted Manuscripts* in the [Information for Authors](#).

Please note that technical editing may introduce minor changes to the text and/or graphics, which may alter content. The journal's standard [Terms & Conditions](#) and the [Ethical guidelines](#) still apply. In no event shall the Royal Society of Chemistry be held responsible for any errors or omissions in this *Accepted Manuscript* or any consequences arising from the use of any information it contains.

Photoisomerization and reorientational dynamics of DTDCI in AOT/alkane reverse micelles containing non-aqueous polar liquids

Manika Dandapat and Debabrata Mandal*

Department of Chemistry, University of Calcutta, 92, APC Road, Kolkata 700 009, India

E-Mail: dmandal.chemistry@gmail.com

Abstract

Molecular mobility of the symmetric carbocyanine fluorophore DTDCI was studied in AOT/alkane reverse micelles containing non-aqueous polar liquids DMF, Formamide, Ethylene Glycol and Glycerol, by monitoring both the torsional photoisomerization and rotational reorientation, both of which were sensitive to microviscosity of the local environment. The DTDCI fluorophore resides completely within the AOT-polar liquid reverse micelle nano-droplets, where its dynamics was found to be significantly retarded irrespective of the polar liquid taken, due to a combination of electrostatic and hydrophobic forces that induce the guest DTDC⁺ cation to attach to the AOT molecules of the host droplet. Addition of strong hydrogen-bond donating polar liquids like Formamide, Ethylene Glycol and Glycerol causes a systematic enlargement of the droplets. Rotational dynamics of the fluorophore inside the nano-droplets was characterized by a diffusion coefficient comparable to that in high viscous solvents like Ethylene Glycol.

Keywords: AOT microemulsions, non-aqueous polar liquids, hydrodynamic radius, photoisomerization, rotational reorientation

1. Introduction

A reverse micelle (RMs) is an aggregate of surfactant molecules like AOT (sodium bis-ethylhexylsulfosuccinate) that forms in non-polar solvents like alkanes. In the aggregate, the polar head-groups of the surfactants point inward while the hydrocarbon chains point outward, towards the nonpolar solvent (Fig. 1a). Addition of polar liquids to AOT reverse micelles often leads to the formation of stable, optically isotropic liquid solutions called microemulsions¹⁻³. In fact, a polar liquid immiscible with non-polar solvents can get encapsulated inside the RMs, the most common example being water¹⁻³. In recent times, the scope of such encapsulation has widened dramatically to include polar liquids like glycerol (GY)³⁻⁷, ethylene glycol (EG)^{3-6,8-11}, propanediol^{11,11}, formamide (FA)^{3-6,10,12}, dimethylformamide (DMF)^{3,5,6,11}, dimethylacetamide^{3,5,6}, methanol^{10,13-18} and acetonitrile^{10,15-18}. In these systems, the polar liquid remains dispersed as AOT-coated droplets in the non-polar solvent. These droplets often exhibit a systematic variation of size with the ratio $w' = [\text{polar liquid}]/[\text{AOT}]$. While AOT RMs at $w' = 0$ consist of droplets with hydrodynamic diameter (d_h) of about 3 nm¹⁹, those laden with ethylene glycol or formamide may attain d_h of 9 - 12 nm even at $w' = 2$ ³.

Thus, AOT reverse micelles and microemulsions open up exciting prospects for physico-chemical processes confined in a nano-dimensional droplet. Consequently, they have proved to be important in spectroscopy^{5,6,11-18,20-22}, catalysis²²⁻²⁴, biochemistry²³⁻²⁵ and nanoparticle fabrication²⁶⁻²⁸. In particular, fluorescence spectroscopy has been widely used to study processes like solvation dynamics^{7,12, 15-17}, charge-transfer¹⁶⁻¹⁸, proton transfer²⁰, energy transfer²¹ in AOT reverse micelles containing water or other polar liquids. The general consensus is that spacial restriction of a polar liquid in a nano-dimensional droplet strongly perturbs the local environment, which is characterized by a markedly slower dynamics and lower polarity compared to the bulk polar solvents.

While water is known to produce well-defined water-pools within the RM, FTIR and ¹HNMR spectroscopy have revealed that non-aqueous polar liquids exhibit a much more complicated behavior depending on their hydrogen-bonding capacities. For example, the potent hydrogen-bond donor GY solvates the AOT head-group via hydrogen-bonding with the SO₃⁻, eventually forming a well-defined pool inside the RM, just like water²⁹. However, in case of EG - also a good H-bond donor - no evidence of liquid pool emerges even at $w' = 2$ or 4. Rather, EG hydrogen-bonds with the carbonyl group of AOT and penetrates into the oil side of interface^{3-5,29-}

³¹. On the other hand, FA is known to produce the largest droplets for a given w' -value, although it is a much smaller molecule than either EG or GY. It has been proposed that FA interacts electrostatically with AOT anion, effectively replacing the Na^+ counterion from the interface. This causes an increase in the effective AOT head-group area and droplet size ^{3,12,32,33}.

In this paper, we present our results on the study of the molecular motion of the fluorophore 3,3'-Diethylthiadicarbocyanine iodide (DTDCI, Fig. 1b) in AOT/alkane based RMs containing four different polar liquids: DMF, FA, EG and GY. DTDCI belongs to the family of symmetric carbocyanines, which have been known to undergo photoisomerization via torsion around one of the C-C bonds in the cyanine bridge³⁶⁻⁴⁷. Since this torsion involves large amplitude motion, photoisomerization of DTDCI is decelerated in high viscous solvents, which results in longer fluorescence life-times ⁴⁷. In fact, the photoisomerization rate constant k_{iso} and the solvent viscosity (η) were found to be empirically related as:

$$k_{\text{iso}} \propto 1/\eta^a \quad (1)$$

where a is an adjustable parameters, with $0 \leq a \leq 1$ ^{35,45,47}. In recent times, several groups have also reported on symmetric carbocyanine fluorophores confined in supramolecular assemblies like micelles ^{34,38,40,45}, reverse micelles ^{34,37,47}, liposomes ⁴⁶, etc., where the photoisomerization rates were found to be remarkably suppressed. This was attributed to high "microviscosity" in these media, which exerts frictional resistance on molecular mobility of the fluorophore. Since this friction is generated by localized interactions operating between the fluorophore and molecules in its immediate vicinity, the measured microviscosity reflects on the nature of the local environment around the fluorophore. It may be noted here that microviscosity in these solutions is distinct from their bulk viscosity, which are comparable to those of low viscosity liquids.

Earlier, we had found that DTDCI in AOT/water/n-heptane reverse micelles is subjected to high microviscosity, which inhibited both its photoisomerization and rotational reorientation ⁴⁷. In this paper, we attempt to extend our studies to AOT/n-heptane reverse micelles containing other polar liquids.

2. Experimental

DTDCI (3,3'-diethylthiadicarbocyanine iodide) was purchased from Alfa-Aesar. The AOT was dried in vacuo over P₂O₅. All solvents used for spectroscopy were of spectroscopic grade (UV grade, E. Merck). AOT reverse micelles were prepared with 0.1M AOT solution in n-heptane, followed by addition of requisite amount of polar liquids different values of $w' = [\text{polar liquid}]/[\text{AOT}]$. Absorption and fluorescence spectra of the DTDCI solutions were measured in a Shimadzu UVPC-3200 spectrophotometer and a PerkinElmer LS55 fluorimeter, respectively. Picosecond fluorescence dynamics studies of the solutions were conducted with a Horiba JobinYvon Fluorocube-01-NL time correlated single photon counting (TCSPC) setup employing laser diodes operating at a $\lambda_{\text{ex}} = 634$ nm with a repetition rate of 1 MHz, as excitation source. The overall temporal and spectral resolutions of the instrument were ~ 150 ps and ~ 4 nm, respectively. All spectroscopic measurements were performed at 22°C.

3. Results and discussion

a) Photoisomerization and microviscosity

The fluorescence spectra of DTDCI in AOT/n-heptane RMs are generally red-shifted compared to those in the bulk solvents DMF, FA, EG and GY, as shown in Fig. 2. Since DTDCI is hardly soluble in n-heptane, the fluorescence emerges entirely from DTDCI residing within the AOT-polar liquid nano-droplets. Therefore, considering the spectral shift, we can safely conclude that the local microenvironment of DTDCI inside the droplets is different from that in the bulk polar solvents. However, for EG and GY, the RM spectra tend to coincide with the bulk solvent spectra, especially at high w' -values. Absorption spectra of DTDCI (not shown here) were also recorded to confirm that it does not form dimers/ aggregates in these media.

The fluorescence transient curves of DTDCI were recorded in AOT/n-heptane RMs containing DMF, FA, EG and GY at different w' and in the bulk solvents. The curves for FA and EG are shown in Fig. 3a and 3b as representative examples. Single-exponential fitting was adequate for all the curves in both RMs and bulk solvents:

$$I(t) = I(0) \exp(-t/\tau) \quad (2)$$

The lifetimes obtained by fitting are given in Table 1. For each polar liquid, we note that the DTDCI lifetimes in RMs are always substantially longer than that in the corresponding bulk

solvent. From the fluorescence quantum yields and lifetimes, the radiative and non-radiative decay rate constants of DTDCI in the different solutions were calculated as:

$$\begin{aligned} k_{\text{rad}} &= \phi/\tau \\ k_{\text{non-rad}} &= (1-\phi)/\tau \end{aligned} \quad (3)$$

For typical organic fluorophores, the in-built route for non-radiative decay is internal conversion or IC. However, for symmetric carbocyanines, photoisomerization is widely accepted to be a major channel for non-radiative decay, so that:

$$k_{\text{non-rad}} = k_{\text{IC}} + k_{\text{iso}} \quad (4)$$

Aramendia et al. measured the ϕ values of several carbocyanines in various solvents over a broad temperature range and found that $k_{\text{rad}}/(k_{\text{rad}} + k_{\text{IC}}) = 1$ for many of them, including DOCI and DODCI³⁵. This implies $k_{\text{IC}} = 0$, immediately leading to $k_{\text{non-rad}} \approx k_{\text{iso}}$. However, for DTDCI, they determined $k_{\text{rad}}/(k_{\text{rad}} + k_{\text{IC}}) = 0.65$, irrespective of solvent. Putting this value in eq.(3) and (4), we calculated k_{iso} of DTDCI in different solutions, listed them in Table 1, and further plotted them against the respective w' -values in Fig. 3c. We first note that the k_{iso} in pure solvents DMF, FA, EG and GY show a monotonic decrease with increasing solvent viscosity, as expected for a photoisomerizing system undergoing torsion. Secondly, the k_{iso} in the RMs are typically very low: lying within the range of k_{iso} in high-viscous solvents like EG and GY. Thirdly, the k_{iso} in the RMs are almost independent of w' -value.

As noted above, the fluorescence emerging from the RMs derives only from DTDCI lodged inside the AOT/polar liquid nano-droplets. Also, single-exponential nature of the fluorescence decays strongly suggests that the local environment inside the droplets is uniform. Previous studies have indicated that the internal structure of the AOT-polar liquid nano-droplet depends profoundly on the nature and amount of polar liquid added. For FA and GY, liquid pools form inside the droplets, while for EG, the AOT-polar liquid interface is blurred^{1,3}. However, for a given polar liquid, DTDCI appears to register a uniform, high microviscosity inside the nano-droplets, irrespective of w' -value. These observed facts imply that the guest DTDCI fluorophore is strongly associated with the AOT molecules of the host droplet, something which the added polar liquid is unable to break significantly. Such a condition may be realized as depicted in Figure 1a: the large hydrophobic part of the rod-like DTDC⁺ cation lies buried among the hydrocarbon tails of the AOT molecules of the RM due to favorable

hydrophobic interactions, while the cationic charge is held by strong electrostatic attraction to the $-\text{SO}_3^-$ anion at the AOT head-group. The collective effect is a marked decrease in DTDCI mobility.

b) Rotational Reorientation

Time-resolved fluorescence anisotropy $r(t)$ of a fluorophore is given by:

$$r(t) = [I_{\parallel}(t) - I_{\perp}(t)] / [I_{\parallel}(t) + 2I_{\perp}(t)] \quad (5)$$

where $I_{\parallel}(t)$ and $I_{\perp}(t)$ are the temporal fluorescence intensities recorded at emission polarizations oriented parallel and perpendicular, respectively, to the exciting light pulse. The $r(t)$ of DTDCI in the AOT RMs and bulk polar solvents were recorded, and plotted in Fig. 4. With increase in w' , the $r(t)$ curve of DMF remains almost invariant, but those for FA, EG and GY all become distinctly slower. Fluorescence anisotropy loss in nanosecond time-scales is generally attributed to the rotational reorientation of the fluorophore molecule as a whole⁴⁸, which is also dependent on the microviscosity. Thus at first sight, the $r(t)$ curves in Fig. 4 are quite puzzling, since they seem to suggest that microviscosity inside the nano-droplets is increasing monotonically with increasing w' -value. In contrast, the photoisomerization rate constants inside the nano-droplets had displayed no systematic or significant variation with increasing w' -value (see Table 1 and Fig. 3c). This apparent contradiction could be resolved once we factored in the rotational motion of the entire nano-droplet.

The overall fluorescence anisotropy of a fluorophore embedded in a rotating nano-droplet is given by⁴⁹:

$$r(t) = 0.4 \times r_f(t) \times r_{\text{drop}}(t) \quad (6)$$

where $r_f(t)$ and $r_{\text{drop}}(t)$ are the fluorescence anisotropies of the fluorophore itself, and the carrier nano-droplet, respectively. The nano-droplet itself is a nearly spherical particle suspended in the non-polar solvent, and having an inherent rotational motion characterized by the time-constant:

$$\tau_{\text{drop}} = (4/3)\pi r_h^3 \eta / k_B T$$

where r_h is the hydrodynamic radius of the sphere, and η is bulk viscosity of the non-polar solvent. Then

$$r_{\text{drop}}(t) = \exp(-t/\tau_{\text{drop}})$$

DLS measurements have been used to estimate the hydrodynamic radii of nano-droplets containing polar liquids DMF, FA, EG and GY³. The last 3 liquids all display considerable

droplet enlargement with increase in w' , the largest droplet size being found for FA. As an example, Fig. 5 illustrates how just a 4-fold increase in r_h of FA-containing nano-droplets from $w' = 0$ to $w' = 2$ results in a striking ~ 50 -fold increase in τ_{drop} . On the other hand, for DMF³, there was negligible change in r_h with change in w' . Using the bulk viscosity of the non-polar solvent n-heptane, the τ_{drop} for DMF-laden droplets at $w' = 1, 2$ and 3 were calculated as: 1.9, 2.1 and 2.2 ns, respectively. Meanwhile, the $r(t)$ curves for these same DMF-laden droplets in Fig. 4 could be nicely fitted to a single-exponential decay function, yielding rotational time-constants (τ_{rot}) 1.85, 2.0 and 2.15 ns, for $w' = 1, 2$ and 3 , respectively. The close proximity of these τ_{rot} values and their corresponding τ_{drop} values at a given w' immediately gives us a clue to the $r(t)$ behavior of DTDCI in nano-droplets. It stipulates that $r_f(t)$, the fluorescence anisotropy due to the fluorophore DTDCI itself, is an extremely slow-decaying function when DTDCI is trapped within the droplet. Hence time-profile of the overall anisotropy $r(t)$ is essentially determined by that of $r_{\text{drop}}(t)$, which decays with time-constant of τ_{drop} . In other words, rotational reorientation of DTDCI inside the nano-droplet is severely constrained.

We calculated τ_{drop} for AOT nano-droplets containing FA, EG and GY using reported hydrodynamic radius values³, and constructed the corresponding $r_{\text{drop}}(t)$ curves. Then, using Eq. (6), we extracted $r_f(t)$, the anisotropy of the fluorophore itself, independent of the rotation of the carrier nano-droplet. The $r_f(t)$ curves are plotted in Fig. 6, along with $r(t)$ curves of DTDCI in the corresponding bulk polar solvents for a visual comparison of the anisotropy loss. We immediately note that, unlike the overall anisotropy $r(t)$, the anisotropy $r_f(t)$ of DTDCI itself is an extremely slow-decaying function inside the AOT-polar liquid nano-droplet, virtually independent of $w' = [\text{polar liquid}]/[\text{AOT}]$. However, the $r_f(t)$ kinetics does depend on the choice of polar liquid. For GY-laden droplets $r_f(t)$ remains nearly constant, but for FA- and EG-laden droplets, it shows a hindered rotor-like decay feature⁴⁹. Such systems are best treated with the wobbling-in-cone model^{45,49}, where the fluorophore is thought to be executing two simultaneous but distinct types of motion inside the droplet : wobbling within a limited conical volume element, and lateral diffusion across the surface of the droplet. This requires that $r_f(t)$ be fitted with a double-exponential decay function of the form:

$$r_f(t) = (1-\beta)\times\exp(-t/\tau_{\text{fast}}) + \beta\times\exp(-t/\tau_{\text{slow}}) \quad (7)$$

where the fitting time-constants τ_{fast} and τ_{slow} are associated with the time-constants for wobbling (τ_w) and lateral diffusion (τ_{lat}) as:

$$1/\tau_{\text{fast}} = 1/\tau_w + 1/\tau_{\text{slow}}$$

$$\text{and, } 1/\tau_{\text{slow}} = 1/\tau_{\text{lat}} \quad (8)$$

The semi-cone angle θ of the conical volume element and diffusion constant for wobbling (D_w) are given by:

$$\sqrt{\beta} = 0.5 \cos\theta (1 + \cos\theta) \quad (9)$$

and

$$D_w = \tau_w^{-1}(1 - \beta)^{-1} [\{\ln((1+q)/2) + (1-q)/2\}q^2(1+q)^2/2(q-1) + (6+8q-q^2-12q^3-7q^4)(1-q)/24] \quad (10)$$

(where $q = \cos\theta$)

Obviously, knowledge of θ and D_w gives vital insight into the spatio-temporal constraints imposed on DTDCI embedded in the nano-droplet.

We fitted the $r_f(t)$ curves of DTDCI in FA- and EG-laden nano-droplets and calculated τ_w , τ_{lat} , θ and D_w in them. The results, listed in Table 2, indicate that DTDCI is forced to wobble within a semi-cone angle of only $\sim 25^\circ$, with a wobbling diffusion constant of $\sim 2.0 \times 10^7 \text{ s}^{-1}$. Also, note that θ and D_w do not vary noticeably as the w' is varied. In contrast, for DTDCI in water-containing reverse micelles⁴⁷, θ is nearly two-fold wider ($\sim 40^\circ$), while D_w lies in the range of $7.0 - 10.0 \times 10^7 \text{ s}^{-1}$, as the water content is increased from $w' = 12$ to $w' = 30$. Moreover, the lateral diffusion time-constants for DTDCI in FA- and EG-laden nano-droplets ($\sim 20 \text{ ns}$) are almost twice as slow than those in water-laden nano-droplets (5- 9 ns)⁴⁷. In other words: spatio-temporal constraints in water-containing nano-droplets are considerably lower.

The photoisomerization results presented earlier in this paper had suggested that the DTDC⁺ guest cation remains steadfastly associated with the AOT molecules of the host nano-droplet by a favorable combination of hydrophobic forces and electrostatic attraction with the anionic $-\text{SO}_3^-$ head-groups of AOT. When DMF is added, the situation does not change much, since DMF fails to solvate the AOT head-groups due to its weak H-bond donor acidity. On the other hand, addition of FA and EG certainly perturbs the nano-droplet interior, since both these liquids strongly interact with the AOT molecules. This helps to dis-engage some of the DTDCI molecules from the AOT, decreasing the constraints on their motion. However, their mobility is still much lower than that in water-containing nano-droplets because (i) water is a much better H-bond donor than FA⁵⁰ and can solvate the $-\text{SO}_3^-$ anion of AOT more efficiently, (ii) although H-bond acidity of EG is only slightly lesser than that of water⁵⁰, EG is known to interact

preferably with the carbonyl group of AOT¹ rather than the $-\text{SO}_3^-$ group responsible for electrostatic forces attracting and restraining the DTDC^+ cation. As a consequence, neither EG nor FA are as effective as water in promoting the mobility of the guest molecules. Hence, torsional photoisomerization as well as wobbling and lateral diffusion of DTDCI are all slower in FA- and EG-containing nano-droplets compared to their water-containing counterparts. In case of GY-laden nano-droplets, the situation is somewhat problematic. Here, both torsion and rotational relaxation of DTDCI molecules remain drastically inhibited despite the fact that GY is a strong H-bond donor known to solvate the AOT sulfonate head-groups efficiently¹. A possible explanation is as follows: each GY molecule possesses 3 $-\text{OH}$ groups. Inside the droplets, the GY molecules crowd at the interface with AOT, where each GY uses one of its $-\text{OH}$ groups to donate H-bonds to the $-\text{SO}_3^-$ anion of one AOT molecule. However, the electron-rich O atoms of the two remaining $-\text{OH}$ groups can still attract any electron-deficient species lying at the interface, like the DTDC^+ cation. In that case, even after addition of GY, the DTDCI molecules remain constrained since they are now tethered to the GY molecules at the interface instead of the AOT molecules.

Finally, the $r(t)$ curves of DTDCI in the bulk solvents DMF, FA, EG and GY were subjected to straightforward single-exponential decay fitting, yielding rotational time constants (τ_{rot}) of 0.33, 0.75, 3.5 and 21 ns, respectively. The diffusion constant for the fluorophore rotating freely in such a homogeneous liquid solvent medium is simply⁴⁹:

$$D_{\text{rot}} = 1/(6 \times \tau_{\text{rot}}) \quad (11)$$

Thus, D_{rot} for DTDCI rotating in the bulk solvents display a ~ 50 fold variation from $50.5 \times 10^7 \text{ s}^{-1}$ in DMF to $0.8 \times 10^7 \text{ s}^{-1}$ in GY. In particular, $D_{\text{rot}} = 22.5 \times 10^7 \text{ s}^{-1}$ and $4.8 \times 10^7 \text{ s}^{-1}$ in bulk FA and EG, respectively. It is instructive to note that the wobbling diffusion rates of the DTDCI fluorophore confined inside the nano-droplets are comparable to its free rotational diffusion rates in bulk high-viscosity liquids EG and GY.

4. Conclusion

Due to its insolubility in alkanes, the DTDCI molecule in AOT reverse micelle solutions resides exclusively within the AOT-polar liquid nano-droplets and is expected to probe the local environment in terms of the microviscosity, i.e., molecular friction resisting its mobility. We examined two different forms of motion: torsional photoisomerization and rotational

reorientation. We had chosen the polar liquids over a very wide range of bulk viscosity (0.3 mPa.s for DMF to 930 mPa.s for glycerol). Although the DTDCI photoisomerization rate constants (k_{iso}) decrease monotonically with viscosity in the bulk solvents, k_{iso} inside the AOT droplets display only minor dependence on the choice of polar liquid and deviate only slightly from that in the $w' = 0$ reverse micelles (containing no added polar liquid). On the basis of these observations, we conjecture that the DTDCI is predominantly associated with the AOT molecules of the droplets, through a favorable combination of electrostatic and hydrophobic interactions.

The role of the polar liquid apparently becomes more prominent in the rotational reorientation experiments, where the size-enlargement of the nano-droplets at high values of $w' = [\text{polar liquid}]/[\text{AOT}]$ seems to slow down the fluorescence anisotropy decay. However, once the results are corrected for this size-enlargement, the rotational dynamics of the fluorophore itself, lodged inside the nano-droplet, was found to be an extremely slow decaying function at all values of w' . In fact, according to the wobbling-in-cone model, the DTDCI fluorophore is forced to wobble inside the droplet within a rather narrow conical volume element limited by a semi-cone angle of only $\sim 25^\circ$, with a diffusion constant $D_w \sim 2 \times 10^7 \text{ s}^{-1}$. The fact that $\theta \ll 360^\circ$ and D_w is similar to the free rotational diffusion constants in high viscous solvents like ethylene glycol and glycerol emphasizes the spacio-temporal restrictions operating on the fluorophore mobility inside the droplets.

Finally, we note that our data corroborates the size-enlargement of nano-droplets previously reported from results of DLS experiments^{1,3}. However, this enlargement is a consequence of AOT-polar liquid interactions which also causes drastic changes within the internal structure of the droplets. Curiously, our data is insensitive to these internal changes, since the microviscosity encountered by DTDCI inside the droplets is almost uniform for any added amount of a given polar liquid. Thus, even if the internal structure changes, a given guest fluorophore may fail to register it depending on the relative strength of molecular interactions. In this case, we propose that the AOT-DTDCI interaction is sufficiently strong to be affected significantly by the presence of the added polar liquid.

Acknowledgements

Financial support for the work was obtained from the Council of Scientific & Industrial Research (CSIR), India, under Project No. 01(2390)/10/EMR – II). Time-resolved spectroscopic experiments were carried out at the University of Calcutta with the TCSPC instrument purchased under the DST (FIST Program), India. M.D. thanks University Grants Commission, India for awarding research fellowships.

References

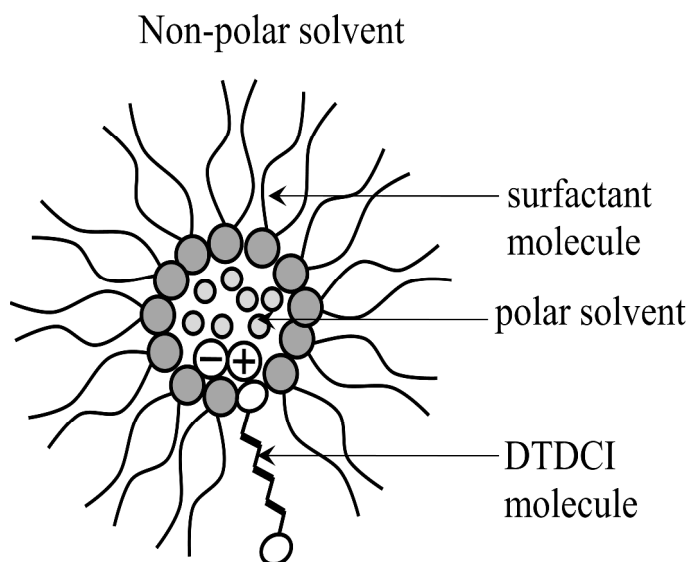
1. N.M. Correa, J.J. Silber, R.E. Riter, N.E. Levinger, Nonaqueous polar solvents in reverse micelle systems, *Chem. Rev.*, 2012, **112**, 4569-4602.
2. I. Danielsson, B. Lindman, The definition of microemulsion, *Colloids Surf.*, 1981, **3**, 391-392.
3. R.D. Falcone, J.J. Silber, N.M. Correa, What are the factors that control non-aqueous/AOT/n-heptane reverse micelle sizes? A dynamic light scattering study, *Phys. Chem. Chem. Phys.*, 2009, **11**, 11096-11100.
4. C.A.T. Laia, P.L-Cornejo, S.M.B. Costa, J. d'Oliveira, J.M.G. Martinho, Dynamic light scattering study of AOT microemulsions with nonaqueous polar additives in an oil continuous phase, *Langmuir*, 1998, **14**, 3531-3537.
5. R.D. Falcone, N.M. Correa, M.A. Biasutti, J.J. Silber, The use of acridine orange base (AOB) as molecular probe to characterize nonaqueous AOT reverse micelles, *J. Colloid Interface Sci.*, 2006, **296**, 356-364.
6. R.D. Falcone, J.J. Silber, M.A. Biasutti, N.M. Correa, Binding of *o*-nitroaniline to nonaqueous AOT reverse micelles, *ARKIVOC*, 2011, **vii**, 369-379.
7. A. Chakraborty, D. Seth, P. Setua, and N. Sarkar, Dynamics of solvent and rotational relaxation of glycerol in the nanocavity of reverse micelles, *J. Phys. Chem. B*, 2006, **110**, 5359-5366.
8. D.G. Hayes, E. Gulari, Ethylene glycol and fatty acid have a profound impact on the behavior of water-in-oil microemulsions formed by the surfactant Aerosol-OT, *Langmuir*, 1995, **11**, 4695-4702.

9. L. Mukherjee, N. Mitra, P.K. Bhattacharya, S.P. Moulik, Kinetics in microemulsion medium. 4. Alkaline fading of crystal violet in aqueous (H₂O/Aerosol OT/Isocetane and H₂O/Aerosol OT/decane) and nonaqueous (ethylene glycol/ Aerosol OT/Isocetane) microemulsions, *Langmuir*, 1995,**11**, 2866-2871.
10. C.A.T. Laia, S.M.B. Costa, Rotational friction in AOT microemulsions: relevance of hydrodynamic and dielectric contributions to microviscosities probed by fluorescent bis[4-(dimethylamino)phenyl] squaraine, *Langmuir*, 2002, **18**, 1494-1504.
11. R.E. Riter, J.R. Kimmel, E.P. Undiks, N.E. Levinger, Novel reverse micelles partitioning nonaqueous polar solvents in a hydrocarbon continuous phase, *J. Phys. Chem. B*, 1997,**101**, 8292-8297.
12. R.E. Riter, E.P. Undiks, J.R. Kimmel, N.E. Levinger, Formamide in reverse micelles: restricted environment effects on molecular motion, *J. Phys. Chem. B*, 1998,**102**, 7931-7938.
13. R. Lu, R. Zhu, R. Zhong, A. Yu, Locations of methanol in methanol-containing AOT reverse micelles revealed by photophysics of IR125, *J. Photochem. Photobiol., A*, 2013, **252**, 116-123.
14. D.S. Venables, K. Huang, C.A. Schmuttenmaer, Effect of reverse micelle size on the librational band of confined water and methanol, *J. Phys. Chem. B*, 2001, **105**, 9132-9138.
15. P. Hazra, N. Sarkar, Solvation dynamics of Coumarin 490 in methanol and acetonitrile reverse micelles, *Phys. Chem. Chem. Phys.*, 2002,**4**, 1040-1045.
16. P. Hazra, D. Chakrabarty, N. Sarkar, Intramolecular charge transfer and solvation dynamics of coumarin 152 in Aerosol-OT, water-solubilizing reverse micelles, and polar organic solvent solubilizing reverse micelles, *Langmuir*, 2002, **18**, 7872-7879
17. P. Hazra, D. Chakrabarty, A. Chakraborty, N. Sarkar, Effect of hydrogen bonding on intramolecular charge transfer in aqueous and non-aqueous reverse micelles, *J. Photochem. Photobiol., A*, 2004, **167**, 23-30.
18. T. Pradhan, H.A.R. Gazi, B. Guchhait, R. Biswas, Excited state intramolecular charge transfer reaction in non-aqueous reverse micelles: effects of solvent confinement and electrolyte concentration, *J. Chem. Sci.*, 2012,**124**, 355-373.
19. R.E. Riter, E.P. Undiks, N.E. Levinger, Impact of counterion on water motion in Aerosol OT reverse micelles, *J. Am. Chem. Soc.*, 1998, **120**, 6062-6067.

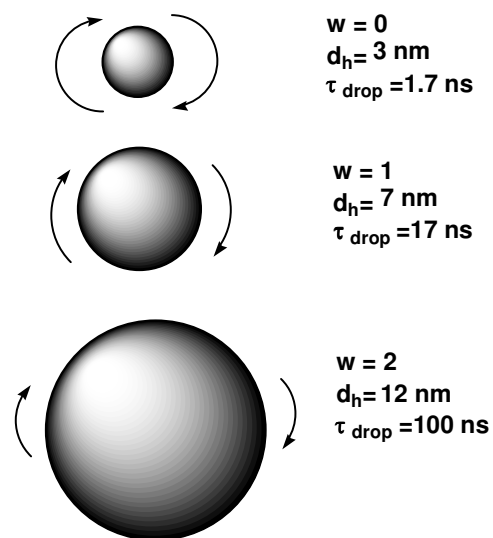
20. S. Basu, S. Mondal, and D. Mandal, Proton transfer reactions in nanoscopic polar domains: 3-hydroxyflavone in AOT reverse micelles, *J. Chem. Phys.*, 2010, **132**, 034701-034706.
21. D. Seth, D. Chakrabarty, A. Chakraborty, N. Sarkar, Study of energy transfer from 7-amino coumarin donors to rhodamine 6G acceptor in non-aqueous reverse micelles, *Chem. Phys. Lett.*, 2005, **401**, 546-552.
22. K. Holmberg, Organic reactions in microemulsions, *Curr. Opin. Colloid Interface Sci.*, 2003, **8**, 187-196.
23. R. V. Rariy, N. Bec, N. L. Klyachko, A. V. Levashov, C. Balny, Thermobarostability of α -chymotrypsin in reversed micelles of aerosol OT in octane solvated by water-glycerol mixtures, *Biotechnol. Bioeng.*, 1998, **57**, 552-556.
24. R. D. Falcone, M. A. Biasutti, N. M. Correa, J. J. Silber, E. Lissi, E. Abuin, Effect of the addition of a nonaqueous polar solvent (glycerol) on enzymatic catalysis in reverse micelles. Hydrolysis of 2-naphthyl acetate by α -chymotrypsin, *Langmuir*, 2004, **20**, 5732-5737.
25. M. A. Biasutti, E. B. Abuin, J. J. Silber, N. M. Correa, E. A. Lissi, Kinetics of reactions catalyzed by enzymes in solutions of surfactants, *Adv. Colloid Interface Sci.*, 2008, **136**, 1-24.
26. M. P. Pileni, Reverse micelles as microreactors, *J. Phys. Chem.*, 1993, **97**, 6961-6973.
27. J. Eastoe, M. J. Hollamby, L. Hudson, Recent advances in nanoparticle synthesis with reversed micelles, *Adv. Colloid Interface Sci.*, 2006, **128**, 5-15.
28. M. P. Pileni, The role of soft colloidal templates in controlling the size and shape of inorganic nanocrystals, *Nat. Mater.*, 2003, **2**, 145-150.
29. O.A. El Seoud, N. M. Correa, L.P. Novaki, Solubilization of pure and aqueous 1,2,3-propanetriol by reverse aggregates of aerosol-OT in isooctane probed by FTIR and ^1H NMR spectroscopy, *Langmuir*, 2001, **17**, 1847-1852.
30. A. M. Durantini, R.D. Falcone, J. J. Silber, N. M. Correa, Effect of the constrained environment on the interactions between the surfactant and different polar solvents encapsulated within AOT reverse micelles, *Chem. Phys. Chem.*, 2009, **10**, 2034-2040.
31. L.P. Novaki, N. M. Correa, J. J. Silber, O.A. El Seoud, FTIR and ^1H NMR studies of the solubilization of pure and aqueous 1,2-ethanediol in the reverse aggregates of aerosol-OT, *Langmuir*, 2000, **16**, 5573-5578.

32. N.M. Correa, N. E. Levinger, What can you learn from a molecular probe? New insights on the behavior of C343 in homogeneous solutions and AOT reverse micelles, *J. Phys. Chem. B*, 2006, **110**, 13050-13061.
33. V. Arcolego, F. Aliotta, M. Goffredi, G. La Manna, V.T. Liveri, Study of AOT-stabilized microemulsions of formamide and n-methylformamide dispersed in n-heptane, *Mater. Sci. Eng. C-Biomimetic Mater. Sens. Syst.*, 1997, **5**, 47-53.
34. S. Basu, S. Mondal, D. Mandal, 3,3'-Diethyloxycarbocyanine iodide: a new microviscosity probe for micelles and microemulsions, *Colloids and Surfaces A: Physicochem. Eng. Aspects*, 2010, **363**, 41-48.
35. P.F. Aramendía, R.M. Negri, E.S. Román, Temperature dependence of fluorescence and photoisomerization in symmetric carbocyanines. Influence of medium viscosity and molecular structure, *J. Phys. Chem.*, 1994,**98**, 3165-3173.
36. L. Scaffardi, R.E.D. Paolo, R. Duchowicz, Simultaneous absorption and fluorescence analysis of the cyanine dye DOCI, *J. Photochem. Photobiol., A*, 1997, **107**, 185-188.
37. A. Datta, D. Mandal, S.K. Pal, K. Bhattacharyya, Photoisomerisation near a hydrophobic surface. Diethyloxadicarbocyanine iodide in a reverse micelle, *Chem. Phys. Lett.*, 1997, **278**, 77-82.
38. S. K. Pal, A. Datta, D. Mandal, K. Bhattacharyya, Photoisomerisation of diethyloxadicarbocyanine iodide in micelles, *Chem. Phys. Lett.*, 1998, **288**, 793-798.
39. S.P. Velsko, D.H. Waldeck, G.R. Fleming, Breakdown of Kramers theory description of photochemical isomerization and the possible involvement of frequency dependent friction, *J. Chem. Phys.*, 1983,**78**, 249-258.
40. S. Ghosh, S. Mandal, C. Banerjee, V.G. Rao, N. Sarkar, Photophysics of 3,3'-diethyloxadicarbocyanine iodide (DODCI) in ionic liquid micelle and binary mixtures of ionic liquids: effect of confinement and viscosity on photoisomerization rate, *J. Phys. Chem. B*, 2012, **116**, 9482-9491.
41. P. Vaveliuk, L.B. Scaffardi, R. Duchowicz, Kinetic analysis of a double photoisomerization of the DTDCI cyanine dye, *J. Phys. Chem.*, 1996, **100**, 11630-11635.
42. A.F. Marks, A.K. Noah, M.R.V. Sahyun, Bond-length alternation in symmetrical cyanine dyes, *J. Photochem. Photobiol., A*, 2001,**139**, 143-149.

43. M.M. Awad, P.K. McCarthy, G.J. Blanchard, Photoisomerization of Cyanines. A comparative study of oxygen- and sulfur-containing species, *J. Phys. Chem.*, 1994, **98**, 1454-1458.
44. J. Rodríguez, D. Scherlis, D. Estrin, P.F. Aramendía, R.M. Negri, AM1 study of the ground and excited state potential energy surfaces of symmetric carbocyanines, *J. Phys. Chem. A*, 1997, **101**, 6998-7006.
45. M. Dandapat, D. Ghosh, D. Mandal, Torsional and reorientational motion of a symmetric carbocyanine in alcohols and in aqueous micelle solutions: 3,3'-Diethylthiadicarbocyanine iodide, *J. Photochem. Photobiol., A*, 2013, **276**, 41-49.
46. M.M.G. Krishna, N. Periasamy, Location and orientation of DODCI in lipid bilayer membranes: effects of lipid chain length and unsaturation, *Biochim. Biophys. Acta*, 1999, **1461**, 58-68.
47. M. Dandapat, S. Basu, D. Ghosh, D. Mandal, Photoisomerization and reorientational mobility of symmetric carbocyanines in AOT/alkane/polar solvent microemulsions, *Chem. Phys. Lett.*, 2014, **608**, 113-119.
48. J. R. Lakowicz, Principles of Fluorescence Spectroscopy, 3rd ed., Springer: New York, (2006).
49. D.B. Spry, A. Goun, K. Glusac, D.E. Moilanen, M.D. Fayer, Proton Transport and the Water Environment in Nafion Fuel Cell Membranes and AOT Reverse Micelles, *J. Am. Chem. Soc.*, 2007, **129**, 8122 - 8130.
50. M.J. Kamlet, J.L.M. Abboud, M.H. Abraham, R. W. Taft, Linear solvation energy relationships. 23. A comprehensive collection of the solvatochromic parameters, π^* , α , and β , and some methods for simplifying the generalized solvatochromic equation, *J. Org. Chem.*, 1983, **48**, 2877-2887.

Graphical Abstract

Structure of AOT nano-droplets



Rotational correlation times for AOT nano-droplets containing formamide

Figure Captions

- Fig. 1.** (a) Schematic representation of a reverse micelle nano-droplet (b) Structure of DTDC⁺ (3,3'-diethylthiadicarbocyanine) cation of DTDCI. The iodide counterion has not been shown.
- Fig. 2.** Normalized fluorescence spectra of DTDCI in AOT/n-heptane reverse micelles containing the polar liquids (a) DMF (b) Formamide (c) Ethylene glycol and (d) Glycerol.
- Fig. 3.** Picosecond fluorescence transients of DTDCI in AOT/n-heptane reverse micelles containing the polar liquids (a) Formamide (FA) and (b) Ethylene glycol (EG). (c) Calculated photoisomerization rate constants (k_{iso}) of DTDCI as a function of $w'=[\text{polar liquid}]/[\text{AOT}]$ in different reverse micelles. The k_{iso} in the bulk polar solvents are indicated by the dotted horizontal lines.
- Fig. 4.** Fluorescence anisotropy time-profiles of DTDCI in AOT/n-heptane reverse micelles containing the polar liquids DMF, Ethylene glycol (EG), Glycerol (GY) and Formamide (FA, inset).
- Fig. 5.** $r_f(t)$ time-profiles of DTDCI in AOT/n-heptane reverse micelles containing the polar liquids Formamide (FA), Ethylene glycol (EG) and Glycerol (GY).

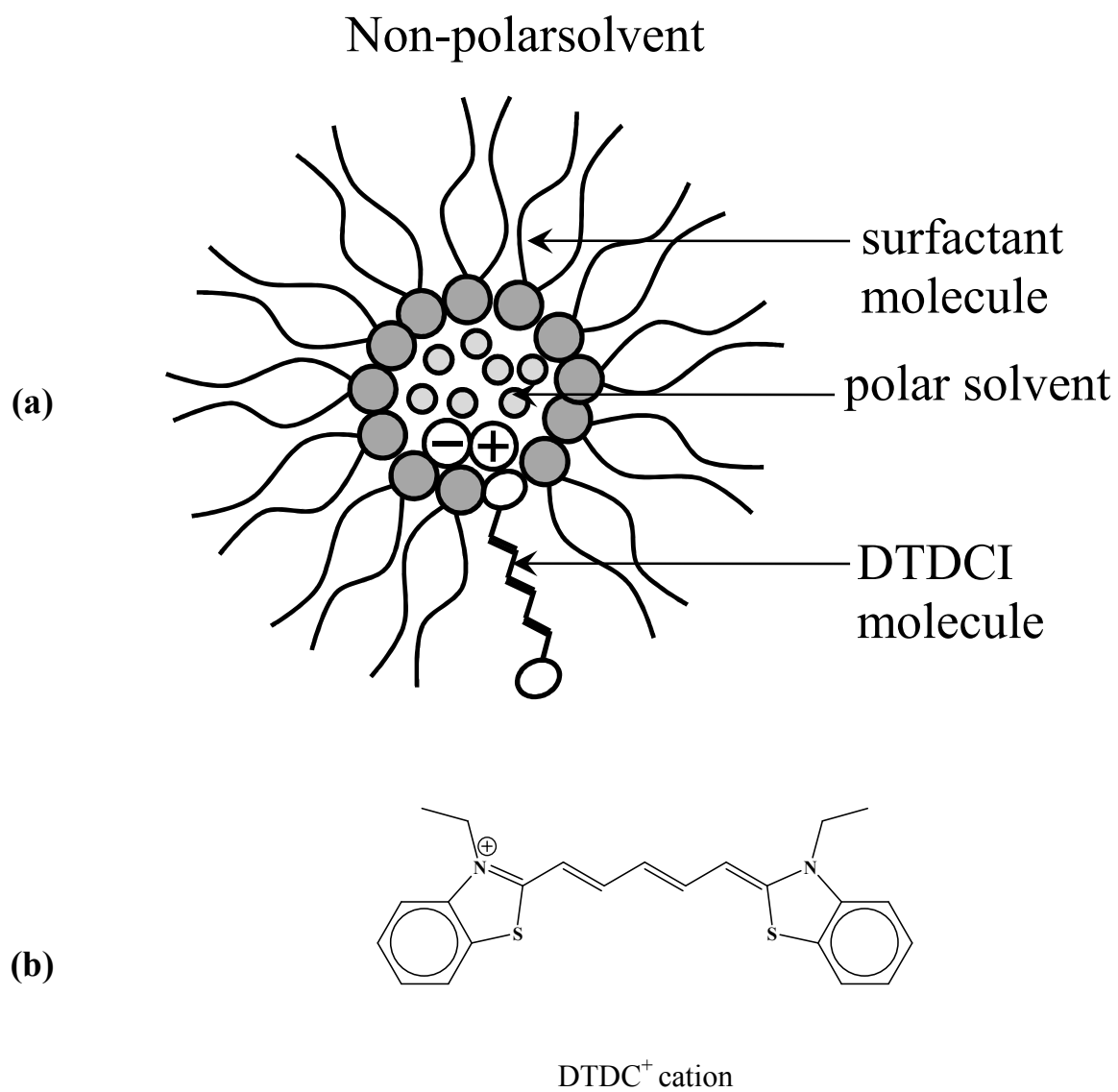


Fig. 1

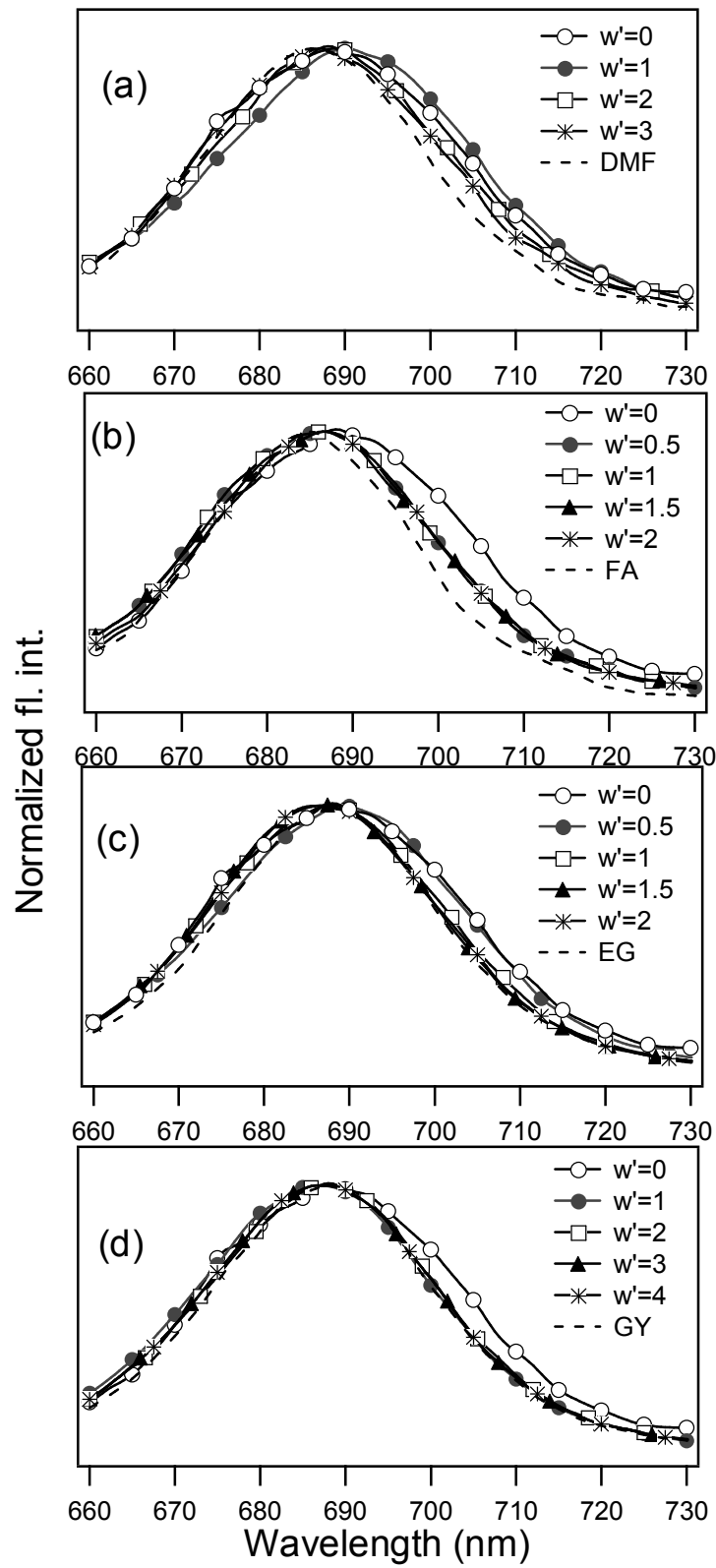


Fig. 2

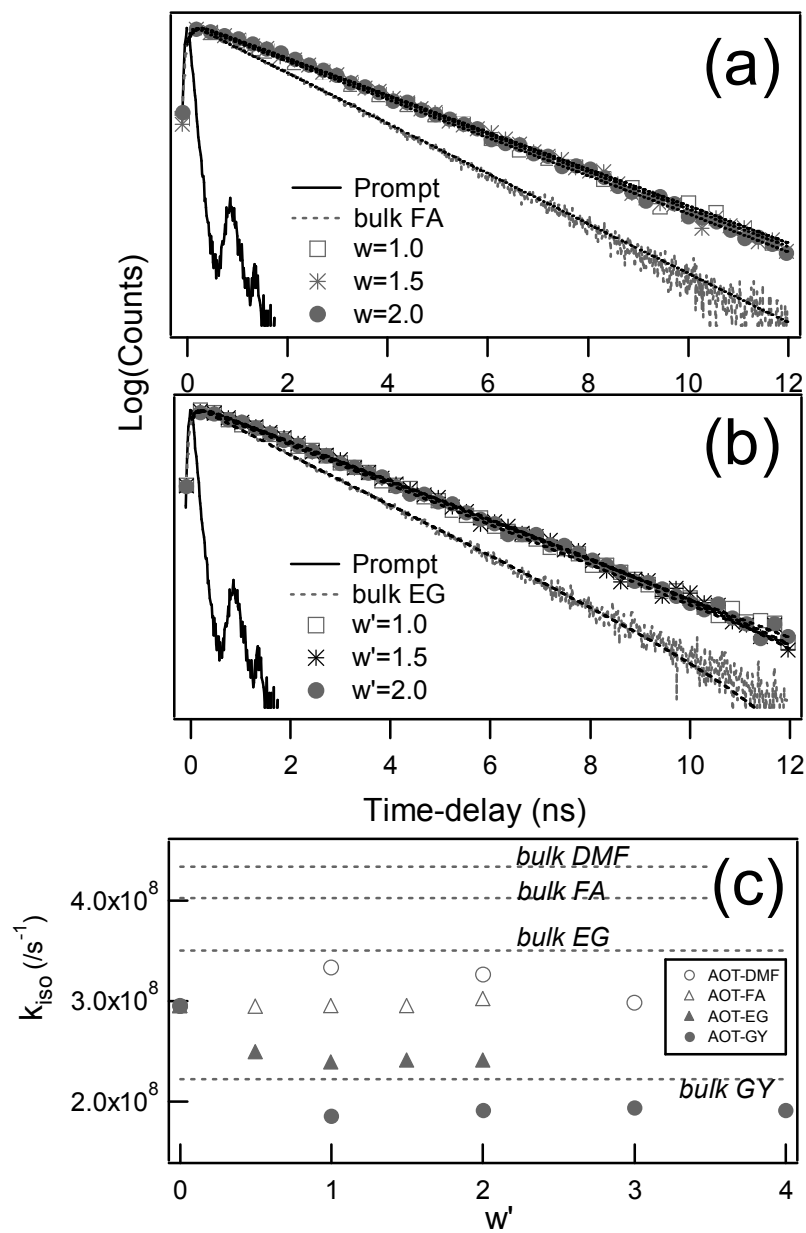


Fig. 3

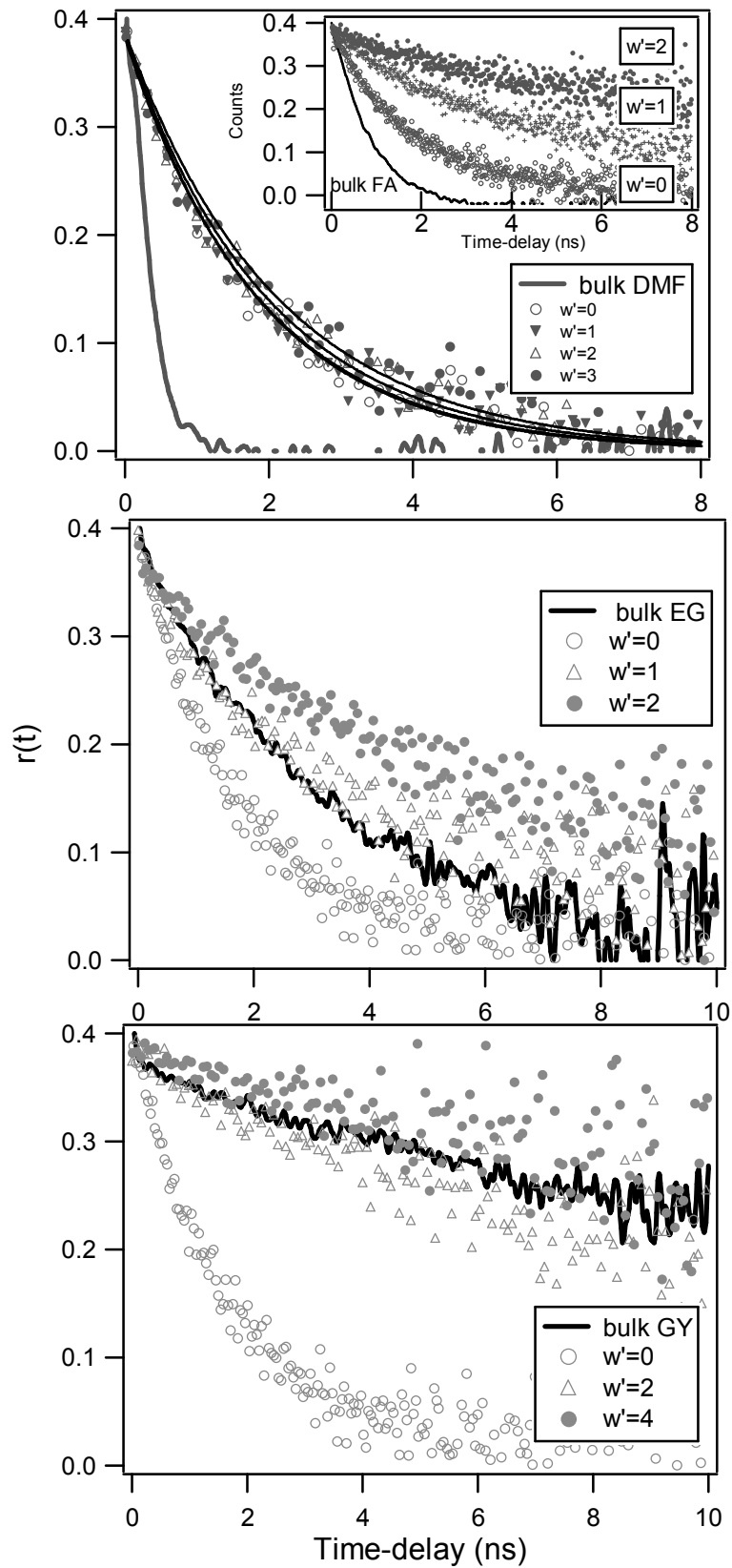


Fig. 4

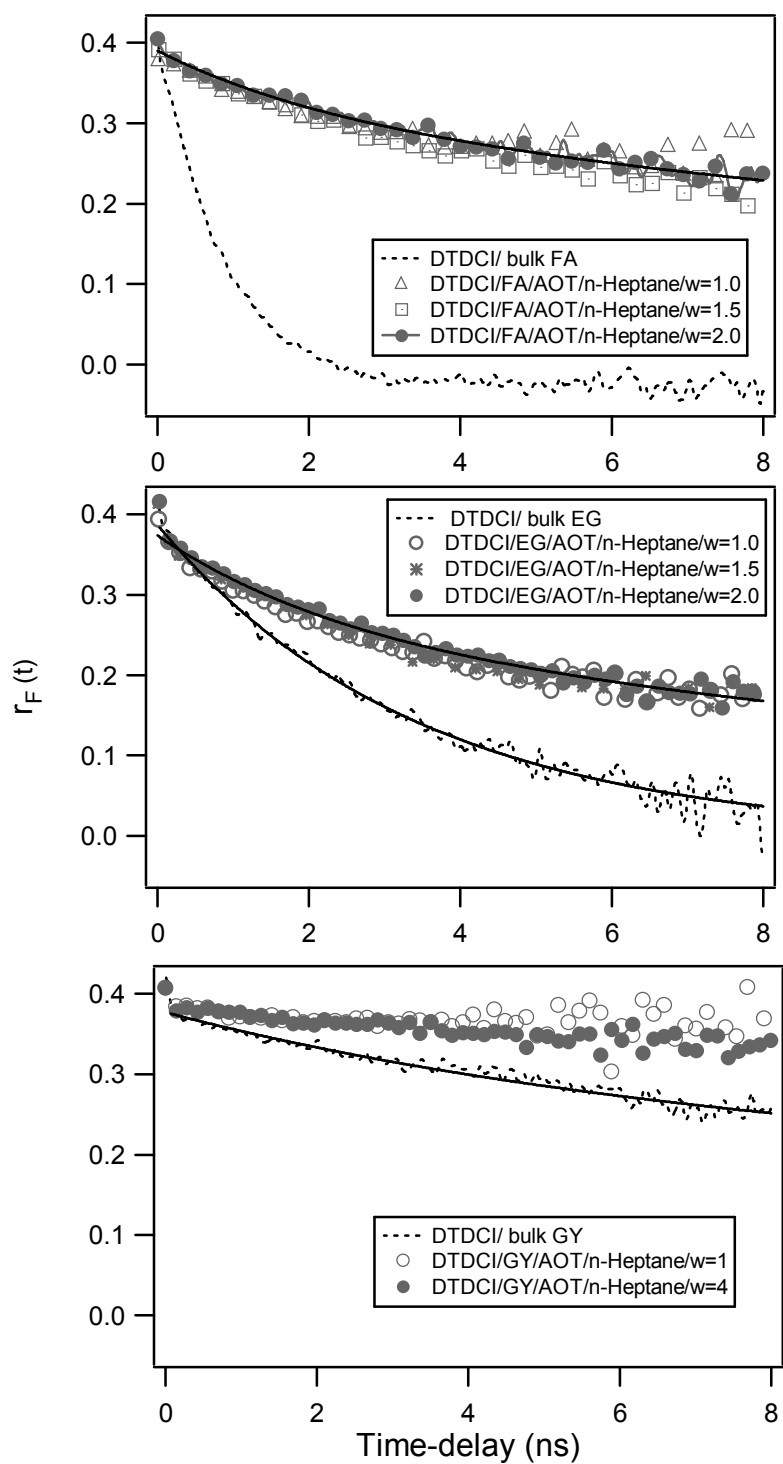


Fig. 5

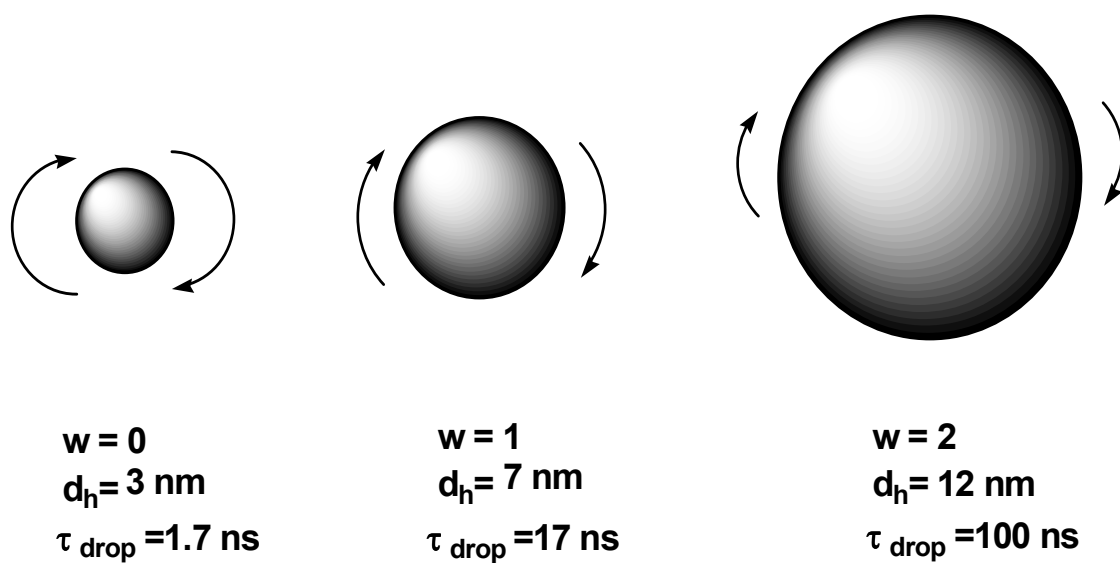


Fig. 6

Table 1. Steady-state and time-resolved spectroscopic parameters of DTDCI in pure bulk solvents and AOT/n-heptane/polar liquid nano-droplets

Polar liquid		Quantum yield ^a (ϕ)	Lifetime (τ /ns)	k_{iso} ($/10^8 s^{-1}$)
None	($w' = 0$)	0.24	2.14 \pm 0.02	2.95
Dimethyl formamide	Bulk solvent	0.20	1.60 \pm 0.01	4.34
	$w' = 1$	0.21	2.04 \pm 0.02	3.33
	$w' = 2$	0.21	2.07 \pm 0.02	3.26
	$w' = 3$	0.21	2.27 \pm 0.02	2.98
Formamide	Bulk solvent	0.21	1.68 \pm 0.02	3.56
	$w' = 0.5$	0.23	2.20 \pm 0.02	2.94
	$w' = 1$	0.22	2.23 \pm 0.02	2.95
	$w' = 1.5$	0.22	2.24 \pm 0.03	2.95
	$w' = 2$	0.21	2.24 \pm 0.03	3.02
Ethylene glycol	Bulk solvent	0.26	1.70 \pm 0.02	3.50
	$w' = 0.5$	0.30	2.16 \pm 0.02	2.49
	$w' = 1$	0.31	2.19 \pm 0.03	2.39
	$w' = 1.5$	0.30	2.24 \pm 0.03	2.41
	$w' = 2$	0.30	2.24 \pm 0.03	2.41
Glycerol	Bulk solvent	0.33	2.22 \pm 0.03	2.22
	$w' = 1$	0.36	2.40 \pm 0.04	1.85
	$w' = 2$	0.34	2.48 \pm 0.04	1.91
	$w' = 3$	0.33	2.55 \pm 0.05	1.93
	$w' = 4$	0.33	2.59 \pm 0.05	1.91

^a Error: $\pm 5\%$

Table 2. Time-resolved anisotropy parameters ^a of DTDCI in AOT/n-heptane/polar liquid nano-droplets

Polar liquid	Wobbling time-constant (τ_w /ns)	Lateral diffusion time-constant (τ_{lat} /ns)	Semi-cone angle (θ)	Wobbling diffusion-constant (D_w /s ⁻¹)
Formamide	2.50	26.00	23°	1.70×10 ⁷
Ethylene glycol	2.75	21.00	28°	2.40×10 ⁷

^a The values are nearly independent of $w' = [\text{polar liquid}]/[\text{AOT}]$ for a given polar liquid